



Published in final edited form as:

ACS Nano. 2021 March 23; 15(3): 4294–4304. doi:10.1021/acsnano.0c07291.

Injectable Biodegradable Polymeric Complex for Glucose-Responsive Insulin Delivery

Jinqiang Wang,

College of Pharmaceutical Sciences, Zhejiang University, Hangzhou 310058, China; MOE Key Laboratory of Macromolecular Synthesis and Functionalization, Department of Polymer Science and Engineering, Zhejiang University, Hangzhou 310027, China; Department of Bioengineering and California NanoSystems Institute, University of California, Los Angeles, California 90095, United States

Zejun Wang,

Department of Bioengineering and California NanoSystems Institute, University of California, Los Angeles, California 90095, United States

Guojun Chen,

Department of Bioengineering and California NanoSystems Institute, University of California, Los Angeles, California 90095, United States; Department of Biomedical Engineering, and the Rosalind & Morris Goodman Cancer Research Center, McGill University, Montreal, Quebec H3G 0B1, Canada

Yanfang Wang,

College of Pharmaceutical Sciences, Zhejiang University, Hangzhou 310058, China

Tianyuan Ci,

Department of Bioengineering and California NanoSystems Institute, University of California, Los Angeles, California 90095, United States

Li Hongjun,

College of Pharmaceutical Sciences, Zhejiang University, Hangzhou 310058, China; Department of Bioengineering and California NanoSystems Institute, University of California, Los Angeles, California 90095, United States

Corresponding Author: Zhen Gu – College of Pharmaceutical Sciences, Zhejiang University, Hangzhou 310058, China; MOE Key Laboratory of Macromolecular Synthesis and Functionalization, Department of Polymer Science and Engineering, Zhejiang University, Hangzhou 310027, China; Department of General Surgery, Sir Run Run Shaw Hospital, School of Medicine, Zhejiang University, Hangzhou 310016, China; Zhejiang Laboratory of Systems & Precision Medicine, Zhejiang University Medical Center, Hangzhou 311121, China; Department of Bioengineering and California NanoSystems Institute, University of California, Los Angeles, California 90095, United States; Jonsson Comprehensive Cancer Center, University of California, Los Angeles, California 90024, United States; guzhen@zju.edu.cn.

Author Contributions

J.W., J.B.B., and Z.G. designed the experiments. J.W., Z.W., G.C., T.C., H.L., X.L., and D.Z. performed experiments. J.W., Z.W., G.C., Y.W., D.Z., A.R.K., Z.Z., H.M., J.B.B., and Z.G. analyzed the data and wrote the paper.

Supporting Information

The Supporting Information is available free of charge at <https://pubs.acs.org/doi/10.1021/acsnano.0c07291>.

¹H NMR characterization of polymers, morphology characterization of complex, insulin release from complex, glucose-dependent solubility of PLL-FPBA, IPGTT result, dose-dependent cytotoxicity in cells, and the dose-dependent blood glucose regulation ability, the biodistribution, and the biocompatibility of complex in mice (PDF)

Complete contact information is available at: <https://pubs.acs.org/10.1021/acsnano.0c07291>

Xiangsheng Liu,

California NanoSystems Institute, University of California, Los Angeles, California 90095, United States; Division of NanoMedicine, Department of Medicine, David Geffen School of Medicine, Los Angeles, California 90095, United States;

Daojia Zhou,

Department of Bioengineering and California NanoSystems Institute, University of California, Los Angeles, California 90095, United States

Anna R. Kahkoska,

Department of Medicine, University of North Carolina School of Medicine, Chapel Hill, North Carolina 27599, United States

Zhuxian Zhou,

Key Laboratory of Biomass Chemical Engineering of Ministry of Education and Center for Bionanoengineering, College of Chemical and Biological Engineering, Zhejiang University, Hangzhou 310027, China;

Huan Meng,

Department of Bioengineering, University of California, Los Angeles, California 90095, United States; Division of NanoMedicine, Department of Medicine, David Geffen School of Medicine, Los Angeles, California 90095, United States; Jonsson Comprehensive Cancer Center, University of California, Los Angeles, California 90024, United States;

John B. Buse,

Department of Medicine, University of North Carolina School of Medicine, Chapel Hill, North Carolina 27599, United States

Zhen Gu

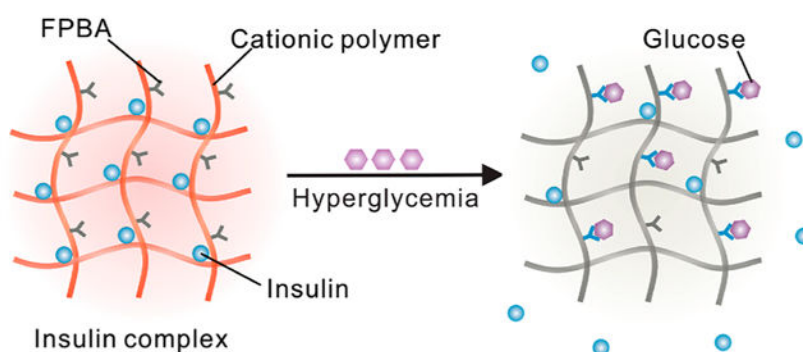
College of Pharmaceutical Sciences, Zhejiang University, Hangzhou 310058, China; MOE Key Laboratory of Macromolecular Synthesis and Functionalization, Department of Polymer Science and Engineering, Zhejiang University, Hangzhou 310027, China; Department of General Surgery, Sir Run Run Shaw Hospital, School of Medicine, Zhejiang University, Hangzhou 310016, China; Zhejiang Laboratory of Systems & Precision Medicine, Zhejiang University Medical Center, Hangzhou 311121, China; Department of Bioengineering and California NanoSystems Institute, University of California, Los Angeles, California 90095, United States; Jonsson Comprehensive Cancer Center, University of California, Los Angeles, California 90024, United States;

Abstract

Insulin therapy is the central component of treatment for type 1 and advanced type 2 diabetes; however, its narrow therapeutic window is associated with a risk of severe hypoglycemia. A glucose-responsive carrier that demonstrates consistent and slow basal insulin release under a normoglycemic condition and accelerated insulin release in response to hyperglycemia in real-time could offer effective blood glucose regulation with reduced risk of hypoglycemia. Here, we describe a poly(L-lysine)-derived biodegradable glucose-responsive cationic polymer for constructing polymer–insulin complexes for glucose-stimulated insulin delivery. The effects of the modification degree of arylboronic acid in the synthesized cationic polymer and polymer-to-insulin ratio on the glucose-dependent equilibrated free insulin level and the associated insulin

release kinetics have been studied. In addition, the blood glucose regulation ability of these complexes and the associated glucose challenge-triggered insulin release are evaluated in type 1 diabetic mice.

Graphical Abstract



Keywords

drug delivery; stimuli-responsive release; diabetes; insulin; glucose-responsive

Diabetes mellitus currently affects more than 463 million people worldwide, and it is estimated to affect more than 700 million people in 2045.¹ Insulin replacement remains essential in treating type 1 and advanced type 2 diabetes.^{1–4} In healthy individuals, endogenous insulin secretion by β -cells of the pancreas oscillates synchronously with the fluctuation of blood glucose levels (BGLs), thereby minimizing both hyper- and hypoglycemia.⁵ Although exogenous insulin replacement strategies are designed to mimic endogenous insulin secretion, the daily administration of injected or infused insulin must be carefully titrated according to an individual's physiology and lifestyle, including changes in stress, physical activity, and dietary intake that may occur day by day.¹ Moreover, excess doses of exogenous insulin can cause life-threatening hypoglycemia, thereby limiting its effectiveness in broad populations.⁶ Therefore, a synthetic system that can mimic β -cells by releasing insulin in a glucose-dependent manner is attractive for facilitating insulin administration by maximizing effectiveness and increasing safety.^{3,7–12} To date, various glucose-responsive insulin delivery systems, such as microneedles,^{13–17} hydrogels,^{18–26} nanoparticles or microparticles,^{27–38} complexes,^{39,40} liposomes,^{41,42} cells,⁴³ and insulin analogues,^{44–46} have been extensively investigated. Among these systems, a glucose-responsive, charge-switchable complex has been validated with robust glucose-responsive performance in animal models.⁴⁰

However, the nonbiodegradable polymer backbone may bring long-term biocompatibility issues. In addition, the normoglycemia state of diabetic mice treated with this formulation only maintained for up to 8 h because of the fast basal insulin release rate, partially arising from the weak interaction between insulin and polymer due to the low molecular weight of the polymer. Therefore, the employment of a biodegradable cationic macromolecule with high molecular weight could potentially solve the biocompatibility issue and enhance the

stability of insulin complex to reduce the basal insulin release rate. In addition, a high glucose stimulation index^{47,48} is also required to mimic the β -cell function for enhancing the blood glucose regulation ability. Because the complicated biological environment could alter the insulin release behavior from the complex, understanding the thermodynamics and kinetics of the *in vitro* glucose-responsive insulin release from complex and the effect of the physical properties of the insulin complex, such as the arylboronic acid-modification degree and polymer-to-insulin ratio, on the relevant *in vivo* glucose stimulation index is essential in guiding the design and preparation of glucose-responsive insulin formulations for clinical translation. Eventually, this investigation could help us connect the *in vitro* glucose-dependent insulin release performance to the *in vivo* blood glucose regulation ability and glucose stimulation index.

Here, we have synthesized cationic polymers by modifying biodegradable poly(L-lysine) (PLL) with 4-carboxy-3-fluorophenylboronic acid (FPBA), a widely used glucose-sensing component.⁴⁹ Subsequently, these polymers are applied to prepare complexes with negatively charged insulin, whose isoelectric point is pH 5.3 to 5.35,⁵⁰ by leveraging electrostatic attraction at physiological pH. Since the driving force for the formation of polyion complex is also associated with the increase of entropy due to release of counterions,⁵¹ the stability of complex formed from positively charged polymer chain and negatively charged insulin could be affected by the molecular weight (MW) of PLL, the FPBA modification degree, the polymer-to-insulin ratio, and the glucose concentration. In the presence of glucose, the binding of FPBA to glucose induces a decrease of the apparent pK_a of FPBA moiety,⁴⁹ thus introducing negative charges into the polymer chain and subsequently reducing the positive charge density. This results in a decreased attraction between polymer and insulin mainly because of a lesser increase of entropy during the formation of complexes, consequently leading to weakened binding between polymer and insulin and triggering insulin release from complexes (Figure 1A,B). When subcutaneously injected in chemically induced type 1 diabetic mice, the complexes deposit under the skin and release insulin slowly under a normoglycemic condition, maintaining euglycemia. Upon intraperitoneal glucose injection to the complex-treated diabetic mice, elevated BGLs trigger insulin release from the subcutaneous complex, resulting in increased plasma insulin levels and correction of hyperglycemia. The impacts of the FPBA-modification degree in the polymer and polymer-to-insulin ratio on the duration of normoglycemia and *in vivo* glucose-responsive performance are investigated.

RESULTS AND DISCUSSION

PLL is abundant in amino groups and was modified with FPBA using the methods previously described (Scheme S1).⁴⁰ The chemical structures of the obtained FPBA-modified PLL (PLL-FPBA) were characterized by ¹H NMR (Figures S1–4). PLL-FPBA could be hydrolyzed to relatively small molecules when exposed to the widely used model enzyme trypsin^{52,53} as confirmed by matrix-assisted laser desorption ionization-time-of-flight mass spectrometry (MALDI-TOF, Figure S5). Insulin complexes were prepared by mixing insulin and PLL-FPBA in an acidic solution (pH = 2), followed by instant adjustment of pH to 7.4. At this physiologically relevant pH, insulin is negatively charged while PLL-FPBA is positively charged, facilitating the generation of a polyion complex. In this study,

we mainly focused on four complexes prepared from PLL-FPBA with an original PLL MW of 30–70 kg/mol. For simplicity, the complexes prepared from insulin and equal or 2-fold weight of PLL_{0.65}-FPBA_{0.35} (with 35% of amino groups reacted with FPBA-NHS) are designated as LL1-insulin and LL2-insulin (LL*n*-insulin: the first L indicated Lower-FPBA content; LL*n*-insulin, the second L indicated L-Lysine; LL*n*-insulin, the *n* indicated the weight ratio of polymer to insulin), while the complexes prepared from insulin and equal or 2-fold weight of PLL_{0.4}-FPBA_{0.6} (with 60% of amino groups reacted with FPBA-NHS) are designated as L1-insulin and L2-insulin (L*n*-insulin: the L indicated L-Lysine), respectively (Table S1). The loading efficiency of insulin was higher than 90% for these four complexes (Figure S6). The micro-sized insulin complex displayed as a floc-like precipitate (Figure 1C). Its morphology was further determined by fluorescence microscopy (Figure 1D, and Figure S7), transmission electron microscopy (TEM), and scanning electron microscopy (SEM) (Figure S8). The hydrodynamic size and zeta-potential of these complex particles were also measured (Table S1).

The glucose-binding ability of the FPBA element in polymers was evaluated in phosphate-buffered saline at pH 7.4 (PBS 7.4) with varying glucose concentrations (100, 200, and 400 mg/dL) (Figure 2A–C). The glucose concentration was measured using a glucose meter by establishing a standard curve (Figure S9). An instant decrease in glucose concentration was observed once the glucose was added to the complex suspension, suggesting fast glucose binding (Figure 2B,C). In addition, the glucose binding to FPBA increased over time for both complexes. LL1-insulin (Figure 2B) showed similar glucose-binding capacity with L1-insulin (Figure 2C) at glucose concentrations of 100 and 200 mg/dL, indicating that the high density of positive charge in PLL_{0.65}-FPBA_{0.35} may facilitate FPBA binding to glucose.^{54,55} Meanwhile, a lower glucose-binding capacity of LL1-insulin than that of L1-insulin was observed at 400 mg/dL glucose solution (Figure 2B,C).

The glucose-responsive insulin release performance of these complexes was evaluated in PBS 7.4 with varying glucose concentrations (Figure 2D–I and Figures S10–11). The insulin concentration was measured using the Coomassie protein assay reagent. PLL-FPBA was poorly soluble in PBS 7.4, so it caused negligible interference (Figures S12–13). Insulin released at a slow rate in PBS 7.4 without glucose and free insulin reached equilibrium at a concentration lower than 50 $\mu\text{g/mL}$ for LL1-insulin, LL2-insulin, L1-insulin, and L2-insulin. Following the addition of glucose to PBS solution, the rate of insulin release and the equilibrated free insulin concentration increased obviously. A higher glucose concentration could lead to more glucose binding to FPBA residuals on polymers, therefore leading to a decreased positive charge density and reduced attraction between the negatively charged insulin and positively charged polymer. Of note, because both PLL-FPBA and complexes were precipitates, the stability of the complex was monitored by measuring the insulin concentrations in the supernatant of the complex suspension. The insulin release performance was further affected by the FPBA-modification degree, polymer-to-insulin ratio, and polymer MW as follows. First, increasing glucose levels promoted insulin release via introducing negative charges, leading to the reduced attraction between polymer chain and insulin. For example, the insulin release from LL1-insulin and L1-insulin reached 80 $\mu\text{g/mL}$ and 140 $\mu\text{g/mL}$ at 100 mg/dL glucose solution within 30 min, respectively, compared to 144 $\mu\text{g/mL}$ and 305 $\mu\text{g/mL}$ at 400 mg/dL glucose solution, respectively (Figure 2E,F).

Second, a higher FPBA content in the polymer meant a lower positive charge density, so the binding of FPBA to glucose could induce a higher degree of the switch of the positive charge. In addition, a higher FPBA content indicated higher glucose binding capability especially at 400 mg/dL glucose solution (Figure 2B,C), therefore introducing more negative charges and promoting greater insulin release. For example, the rate of insulin release from L1-insulin (Figure 2F) exceeded that of LL1-insulin (Figure 2E). A similar trend in insulin release rate was also observed when comparing LL2-insulin with L2-insulin, especially in 400 mg/dL glucose solution (Figure 2H,I). Third, the ratio of polymer to insulin affected the insulin release rate. A higher polymer-to-insulin ratio could achieve a higher binding capacity of polymer to insulin, therefore reducing the basal free insulin level. After increasing the polymer-to-insulin ratio from 1 (for LL1-insulin and L1-insulin) to 2 (for LL2-insulin and L2-insulin), insulin molecules were held by 2-fold positively charged polymer chains, leading to enhanced binding between polymer chains and insulin molecules (Figure 2D,G). This enhanced binding could slow down the release of insulin from the complex and reduce free insulin level in solution. So, the free insulin quantity at equilibrium in LL2-insulin and L2-insulin suspensions was around 50% less than that of their associated counterparts with fewer polymer contents (Figure 2E,F,H,I). Among the four complexes prepared from PLL of 30–70 kg/mol, L2-insulin exhibited the best glucose responsiveness regarding the ratio of free insulin concentrations of the complex suspension with 400 mg/dL glucose solution to that with 100 mg/dL glucose solution. The equilibrated free insulin concentration in the L2-insulin suspension at 400 mg/dL was 108 $\mu\text{g/mL}$, which was almost 10-fold that at 100 mg/dL (Figure 2I). In comparison, other complexes only achieved a ratio of around 2. Finally, the molecular weight of the polymer also had an impact on the insulin release rate and the balanced free insulin level. Compared with LL1-insulin with an original PLL of 30–70 kg/mol, insulin complexes prepared from PLL_{0.57}-FPBA_{0.43} (PLL of 4–15 kg/mol) and PLL_{0.6}-FPBA_{0.4} (PLL of 15–30 kg/mol) had faster insulin release rates and higher balanced insulin levels at various glucose concentrations (Figures S10–11). Of note, the size of the complexes may also affect the insulin release, even though we currently could not control the size of the complex. However, we found that the insulin release from bulk L1-insulin and L2-insulin centrifuged to the bottom of the Eppendorf tube was slowed down as compared to their suspended counterparts (Figures S14–15). This reduced insulin release from the complex with large size may result from the reduced diffusion rate of glucose into the complex and of insulin to the outside.

The *in vivo* blood glucose regulation ability of the insulin complexes was evaluated in C57BL/6J mice with type 1 diabetes induced by streptozotocin (STZ). Based on the preliminary studies, the insulin equivalent dose was determined as 1.5 mg/kg (Figure S16). In each group, five to ten diabetic mice were included. Both the native insulin and complexes were subcutaneously injected. LL1-, LL2-, L1-, and L2-insulin all exhibited a longer retention time than free insulin based on *in vivo* imaging (Figure 3A,B, and Figure S17). After subcutaneous injection, the BGLs of diabetic mice receiving injections of either complexes or insulin all decreased to normoglycemic levels (Figure 3C,D). Theoretically, L1-insulin had the fastest *in vitro* insulin release rate, while LL2-insulin had the slowest insulin release rate, so L1-insulin was expected to achieve normoglycemia fastest while LL2-insulin should be the slowest one. However, the four formulations achieved

normoglycemia in treated mice all at around 0.5 h. This may have arisen from the heterogeneity of insulin sensitivity among diabetic mice and the anesthesia procedure during insulin complex injection. In addition, after injection, the complex could not sense the level of the interstitial glucose immediately because the complexes were suspended in PBS, the absorption of which required a period of time and could delay the establishment of a local biorelevant glucose environment surrounding the complex.

The normoglycemia duration of diabetic mice treated with complexes was affected by several factors. First, the MW of PLL greatly impacted the blood glucose regulation ability of the insulin complexes. For instance, the BGLs of the diabetic mice treated with complexes prepared from insulin and FPBA-modified PLL_{4-15k} (43% FPBA modification) showed BGLs within the normal range for only 5 h and returned to initial hyperglycemic levels 8 h post-treatment (Figure 3C). Increasing the MW of PLL to 15–30 kg/mol did not prolong the normoglycemia time (Figure 3C). However, further increasing the MW of PLL to 30–70 kg/mol achieved a normoglycemic state longer than 10 h in diabetic mice treated with LL1-insulin, while BGLs returned to initial hyperglycemic levels after 43 h post-treatment (Figure 3D). Second, the FPBA-modification degree mattered, especially when there was an equal weight of insulin and polymer in the complex. Compared with LL1-insulin, L1-insulin only achieved normoglycemia for approximately 10 h and gradually returned to initial hyperglycemia 24 h post-treatment (Figure 3D). Third, the ability of complexes with a twofold polymer (LL2-insulin and L2-insulin) to regulate BGLs was enhanced, especially for that prepared from PLL_{0.4}-FPBA_{0.6}. The BGLs of diabetic mice that received treatment with LL2-insulin were maintained below 200 mg/dL for 28 h post-treatment and remained below the initial hyperglycemic levels even 72 h post-treatment (Figure 3D). Similarly, diabetic mice treated with L2-insulin also showed normoglycemia for more than 28 h (Figure 3D), which was significantly longer than that in diabetic mice treated with L1-insulin. While diabetic mice treated with LL1-insulin, LL2-insulin, and L2-insulin all showed lower BGLs than the original BGLs even after 30 h, only LL2-insulin and L2-insulin remained effective after 50 h, though the BGLs were higher than 200 mg/dL. The blood glucose regulation capabilities of these complexes were consistent with the *in vitro* study, in which L1-insulin had the highest while LL2- and L2-insulin had the lowest balanced free insulin levels in 100 mg/dL glucose solution. A high balanced free insulin level could lead to fast insulin release and shorten the normoglycemia period.

Intraperitoneal glucose tolerance tests (IPGTT) were further performed with the four insulin complexes: LL1-insulin, L1-insulin, LL2-insulin, and L2-insulin. Diabetic mice were randomly assigned to each group ($n = 5$). Diabetic mice treated with PBS or healthy mice were used as controls. Glucose (3 g/kg) was intraperitoneally administered at 8 h post-treatment. Upon administration of glucose, BGLs increased rapidly among all mice and returned to the normal range only in the healthy and complexed-treated groups (Figure 4 and Figure S18). However, the associated change in plasma insulin levels varied across the mice receiving different insulin complexes. Plasma insulin levels among mice treated with LL1-insulin increased to an average of 130% compared to an average of 180% for mice treated with LL2-insulin (Figure 4A,B). Compared to the LL1 and LL2 insulin, the insulin complexes prepared from PLL_{0.4}-FPBA_{0.6} (L1 and L2 insulin) showed elevated glucose-responsive insulin release. After glucose administration, the plasma insulin level increased to

230% and 440% at 60 min for L1-insulin and L2-insulin treated diabetic mice, respectively (Figure 4C,D). In addition, the plasma insulin levels also decreased to baseline levels along with the normalization of BGLs at 120 min. Furthermore, the BGLs of mice treated with L2-insulin returned to the normal range faster than that of L1-insulin-treated ones. Of note, the blood insulin levels of diabetic mice treated with L1-insulin at 8 h post-treatment were lower than that of the diabetic mice treated with LL1-insulin and LL2-insulin, which may be associated with the fast insulin release within the 8 h period after L1-insulin injection. This is also consistent with the short euglycemia period in diabetic mice treated with L1-insulin.

Then, *in vitro* cytotoxicity of PLL before and after modification by FPBA was evaluated on L929 cells. PLL_{0.65}-FPBA_{0.35} and PLL_{0.4}-FPBA_{0.6} showed negligible cytotoxicity in the studied concentration range (2 to 500 $\mu\text{g}/\text{mL}$), while unmodified PLL exhibited cytotoxicity at concentrations higher than 50 $\mu\text{g}/\text{mL}$ (Figure S19). The *in vivo* biocompatibility of FPBA-modified PLL was also evaluated. LL2-insulin and L2-insulin prepared with Cy5-labeled polymer were subcutaneously injected, and the biodistribution of polymers was monitored using IVIS spectrum. Both PLL_{0.65}-FPBA_{0.35} and PLL_{0.4}-FPBA_{0.6} were gradually eliminated through the liver from subcutaneous depots within three months after injection (Figures S20–21). Hematoxylin and eosin (H&E) staining results indicated that neutrophil infiltration was localized to the site of the injected complexes (Figure 5A). In addition, the formation of collagen fibers at the injection site was minimal as observed via Masson's trichrome staining (Figure 5B). All insulin complexes were found to be degraded or cleared entirely by three months post-treatment (Figure S20), and no residual collagen fiber deposition was observed (Figure 5B). Furthermore, no significant change has been identified regarding the blood cell counts and serum biochemistry indices (Figures S22–23).

CONCLUSION

In summary, we have prepared various complexes from human recombinant insulin and FPBA-modified PLL with loading efficiency higher than 90%. The complexes were prepared by leveraging the electrostatic attraction between the cationic polymers and insulin as well as the increase of entropy during the formation of polyion complexes. A higher polymer molecular weight, a bigger polymer-to-insulin ratio, and a lower FPBA-modification degree all led to reduced free insulin levels at a normoglycemia-relevant glucose solution. Glucose-stimulated insulin release from complexes was validated and dependent on the polymer MW, FPBA-modification degree, and polymer-to-insulin ratio. Among the complexes studied in this work, L2-insulin exhibited the best glucose-responsiveness regarding the ratio of balanced insulin level in 400 mg/dL glucose solution to that in 100 mg/dL glucose solution. *In vivo* studies in type 1 diabetic mice validated that LL1-insulin, LL2-insulin, L1-insulin, and L2-insulin all had the ability to prolong the antihyperglycemic effect of native insulin, especially for LL2-insulin and L2-insulin, both of which achieved extended normoglycemia for more than 20 h and remained effective even at 72 h post-treatment. Of note, recombinant human insulin was used in these studies. Further evaluation of formulation and dose will be required prior to human studies. This prolonged treatment efficacy is consistent with their ultralow free insulin level in glucose solution at 100 mg/dL. Furthermore, *in vivo* IPGTT-stimulated insulin release performance of subcutaneous L2-insulin depot was found to be the best among the four complexes, which is

in agreement with its highest ratio of balanced free insulin in 400 mg/dL glucose solution to that in 100 mg/dL glucose solution among the complexes in this study. From a biocompatibility perspective, all complexes were shown to be absent from subcutaneous tissue samples after three months, and no obvious biocompatibility issues were identified. Overall, this study aims to clarify the relevance between *in vitro* and *in vivo* glucose-responsive performance. It was found that the differences in insulin release rates and equilibrated free insulin levels across normoglycemic and hyperglycemic conditions were critical for maximizing the *in vivo* glucose-responsive performance of this type of insulin delivery systems.

MATERIALS AND METHODS

Materials.

Poly(L-lysine) hydrobromide with various MW was purchased from Sigma-Aldrich. Dialysis tube membrane (MWCO = 3500 Da) was purchased from Spectrum Laboratories. *N*-Hydroxysuccinimide (NHS) and 4-carboxy-3-fluorobenzenboronic acid (FPBA) were purchased from Fisher Scientific. Recombinant human insulin was purchased from ThermoFisher Scientific (Catalog No. A113811J). Other reagents were purchased from Sigma-Aldrich. NHS ester of FPBA (FPBA-NHS) was prepared as previously described.⁴⁰

Synthesis of FPBA-Modified PLL, with PLL_{0.4}-FPBA_{0.6} (30–70K) as an

Example.—PLL (100 mg) was dissolved in PBS (0.01 M, pH = 7.4, 10 mL), to which FPBA-NHS (120 mg) dissolved in DMSO (5 mL) was added dropwise while the pH was kept around 7. After the addition of FPBA-NHS solution, the reaction was stirred for another 30 min before dialysis in deionized water (4 L). The obtained mixture was lyophilized, and a white solid was obtained. The product was characterized by ¹H NMR to determine the degree of FPBA modification.

Preparation of Insulin Labeled with Rhodamine B (RhB-insulin).—Rhodamine B isothiocyanate (5 mg) was dissolved in DMSO (1 mL) and then added to the insulin solution (0.1 M Na₂CO₃, 50 mg/mL, 2 mL). The mixture was stirred at room temperature for 2 h before dialysis in deionized water (3 × 4 L). After lyophilization, purple RhB-insulin was obtained. Cyanine 5 (Cy5) labeled PLL-FPBA or native insulin was prepared similarly.

Preparation of Insulin Complex, with PLL_{0.4}-FPBA_{0.6} as an Example.—Both native insulin (10 mg/mL) and PLL_{0.4}-FPBA_{0.6} (10 mg/mL) were prepared beforehand. Then, both solutions (100 μL) were mixed and one drop of NaOH (1 N) was added to bring the pH to 7.4. Subsequently, PBS (pH = 7.4, 1 mL) was added, and the mixture was centrifuged to remove unloaded insulin. The final insulin complex was dispersed in PBS (10 mM, pH = 7.4) at 1 mg/mL (insulin equivalent). The complex was used immediately for subsequent experiments. Other complexes with varied polymers or polymer-to-insulin ratios were prepared in a similar procedure. The insulin level in the supernatant was measured using Coomassie protein assay reagent and calculated using a standard curve. The insulin loading efficacy was calculated accordingly.⁴⁰

Characterization of Complex Particles.—Hydrodynamic size and zeta-potential of complexes were measured on a ZETAPALS (Brookhaven Instruments Corporation). The complexes were suspended in PBS with a final insulin concentration of 0.5 mg/mL. The zeta-potential of the complex at various glucose solutions was measured after adding glucose (0.4 g/mL) to complex suspension and incubating for 5 min. Of note, the particles were polydispersed and easy to precipitate, especially after the addition of glucose. Before observing the complex by SEM (ZEISS Supera 40VP) and TEM (T12 Quick CryoEM and CryoET (FEI)), the LL2-insulin complex was centrifuged, and PBS was replaced by deionized water. The concentration of complex was equivalent to 0.5 mg/mL insulin. The TEM sample was stained by phosphotungstic acid (2%).

3-(4,5-Dimethylthiazol-2-yl)-2,5-diphenyltetrazolium Bromide (MTT) Assay.—The L929 murine fibroblast cell line was purchased from ATCC. RPMI 1640 medium was supplemented with heat-inactivated fetal bovine serum (10%), penicillin (100 units/mL), and streptomycin (0.1 mg/mL) and used to grow the cells. For cytotoxicity assay, cells were seeded into a 96-well plate (100 μ L medium, 10,000 cells per well) for 24 h before the addition of polymer solution or suspension in culture medium (100 μ L) with series concentrations. The cells were incubated with polymers for another 24 h. Then, the culture medium was replaced with fresh medium with 0.75 mg/mL MTT (100 μ L) for another 3 h. After the removal of the MTT medium, DMSO (200 μ L) was added. After gently shaking for 10 min, the absorbance of each well was measured at 562 nm using a microplate spectrophotometer. Each polymer concentration was tested in triplicate.

In Vitro Glucose-Binding Ability Study.—Complexes (L1-insulin, LL1-insulin) were suspended in PBS 7.4 (1 mL) with the final suspension containing 1 mg/mL PLL-FPBA. Then, glucose (0.4 g/mL) was added to each vial to obtain initial glucose concentrations of 100, 200, and 400 mg/dL. At predetermined time points, the suspension was obtained, and the glucose concentration was measured using a glucose meter (Clarity, BG1000) with the high limit of 600 mg/dL. A standard curve was established for calibration. The glucose solution with a concentration over 200 mg/dL was diluted in an equal volume of PBS before measurement.

In Vitro Insulin Release Study.—The complex suspension was prepared by adding PBS to the complex. Complex prepared from native insulin and polymer was suspended in PBS (pH = 7.4, 1 mg/mL), and allocated to Eppendorf tubes. Into these tubes, glucose (0.4 g/mL) was added to obtain varied glucose concentrations (0, 100, 200, and 400 mg/dL). These tubes were incubated at 37 °C. At timed intervals, the complex suspension was withdrawn and centrifuged. The clear supernatant was used to measure the insulin concentration using Coomassie protein assay reagent via first establishing a standard curve. Of note, the supernatant of the complex suspension was measured before the addition of glucose and had absorbance almost comparable to blank PBS and was set as the zero point. Moreover, both PLL_{0.4}-FPBA_{0.6} and PLL_{0.65}-FPBA_{0.35} were insoluble in PBS at pH 7.4 with glucose concentrations in the range of 0–400 mg/dL, indicating minimal interference from polymers.

In Vivo Blood Glucose-Regulation Study in Type 1 Diabetic Mice.—All animal procedures were performed following the Guidelines for Care and Use of Laboratory Animals of University of California, Los Angeles. Streptozotocin-induced diabetic mice were purchased from Jackson Laboratory. As we were evaluating the long-term BG regulation ability of the complexes, the mice were fed with a standard diet and exposed to a 12-h light and 12-h dark environment. Mice with BGLs higher than 300 mg/dL were selected for the study. Diabetic mice ($n = 5$ to 10) were allocated to groups treated with native insulin and various complexes. Based on the evaluation of the dose-dependent BG regulation ability of the complexes, the insulin equivalent dose of each complex was determined to be 1.5 mg/kg (43 U/kg). The blood glucose was monitored before and after treatment until the blood glucose returned to initial levels. The blood samples were taken from the tail tips and plasma glucose concentration was measured by a glucose meter (Aviva, ACCU-CHEK).

Intraperitoneal Glucose Injection-Induced Insulin Release Study.—Diabetic mice ($n = 5$) were randomly assigned to be treated with various insulin complexes (1.5 mg/kg). Eight hours post-treatment, these mice were intraperitoneally injected with glucose (3 g/kg). Blood samples (40 μ L) were extracted and transferred into Eppendorf tubes pretreated with EDTA. The blood was collected just before glucose injection and at predetermined timed intervals after the glucose injection. The obtained blood was centrifuged, and the plasma insulin level was quantified using a human insulin enzyme-linked immunosorbent assay (ELISA) test (Invitrogen).

Statistical Analysis.—One-way ANOVA with Tukey post-hoc tests and two-way ANOVA were used to carry out multiple comparisons.

Supplementary Material

Refer to Web version on PubMed Central for supplementary material.

ACKNOWLEDGMENTS

This work was supported by the grants from JDRF (grant no. 3-SRA-2015-117-Q-R) and grants from the start-up packages of UCLA and Zhejiang University.

The authors declare the following competing financial interest(s): Z.G. is a scientific co-founder of Zenomics Inc. J.B.B.s contracted consulting fees are paid to the University of North Carolina by Adocia, AstraZeneca, Dance Biopharm, Eli Lilly, MannKind, NovaTarg, Novo Nordisk, Senseonics, vTv Therapeutics, and Zafgen as well as grant support from Novo Nordisk, Sanofi, Tolerion and vTv Therapeutics. He is also a consultant to Cirius Therapeutics Inc, CSL Behring, Mellitus Health, Neurimmune AG, Pendulum Therapeutics, and Stability Health. He holds stock/options in Mellitus Health, Pendulum Therapeutics, PhaseBio, and Stability Health. He is supported by a grant from the National Institutes of Health (UL1TR002489, U01DK098246, UC4DK108612, U54DK118612), PCORI and ADA. A.R.K. received travel support from Novo Nordisk to present data.

REFERENCES

- (1). Lisa D; Andreia F. d. M.; Silvia G. d. L.; Lucy H; Esther J; Abha K; Jinnan L; Inga P; Lorenzo P; Phil R; Els S; Beatriz YJ; Mike W; Wen Y; Jing L; Sue P; Anne WO; Merry RG IDF Diabetes Atlas, 9th ed.; 2019.
- (2). Ohkubo Y; Kishikawa H; Araki E; Miyata T; Isami S; Motoyoshi S; Kojima Y; Furuyoshi N; Shichiri M Intensive Insulin Therapy Prevents the Progression of Diabetic Microvascular

- Complications in Japanese Patients with Non-Insulin-Dependent Diabetes Mellitus: A Randomized Prospective 6-Year Study. *Diabetes Res. Clin. Pract* 1995, 28, 103–117. [PubMed: 7587918]
- (3). Veisheh O; Tang B; Whitehead KA; Anderson DG; Langer R Managing Diabetes with Nanomedicine: Challenges and Opportunities. *Nat. Rev. Drug Discovery* 2015, 14, 45–57. [PubMed: 25430866]
 - (4). Reusch JE; Manson JE Management of Type 2 Diabetes in 2017: Getting to Goal. *JAMA* 2017, 317, 1015–1016. [PubMed: 28249081]
 - (5). Lang D; Matthews DR; Peto J; Turner RC Cyclic Oscillations of Basal Plasma Glucose and Insulin Concentrations in Human Beings. *N. Engl. J. Med* 1979, 301, 1023–1027. [PubMed: 386121]
 - (6). Chantelau E; Spraul M; Muhlhauser I; Gause R; Berger M Long-Term Safety, Efficacy and Side-Effects of Continuous Subcutaneous Insulin Infusion Treatment for Type 1 (Insulin-Dependent) Diabetes Mellitus: A One Centre Experience. *Diabetologia* 1989, 32, 421–426. [PubMed: 2509271]
 - (7). Mo R; Jiang T; Di J; Tai W; Gu Z Emerging Micro- and Nanotechnology Based Synthetic Approaches for Insulin Delivery. *Chem. Soc. Rev* 2014, 43, 3595–3629. [PubMed: 24626293]
 - (8). Yu J; Zhang Y; Bomba H; Gu Z Stimuli-Responsive Delivery of Therapeutics for Diabetes Treatment. *Bioeng. Transl. Med* 2016, 1, 323–337. [PubMed: 29147685]
 - (9). Lu Y; Aimetti AA; Langer R; Gu Z Bioresponsive Materials. *Nat. Rev. Mater* 2017, 2, 16075.
 - (10). Bakh NA; Cortinas AB; Weiss MA; Langer RS; Anderson DG; Gu Z; Dutta S; Strano MS Glucose-Responsive Insulin by Molecular and Physical Design. *Nat. Chem* 2017, 9, 937–943. [PubMed: 28937662]
 - (11). Wang J; Wang Z; Yu J; Kahkoska AR; Buse JB; Gu Z Glucose-Responsive Insulin and Delivery Systems: Innovation and Translation. *Adv. Mater* 2020, 32, No. e1902004.
 - (12). VandenBerg MA; Webber MJ Biologically Inspired and Chemically Derived Methods for Glucose-Responsive Insulin Therapy. *Adv. Healthcare Mater* 2019, 8, 1801466.
 - (13). Yu J; Wang J; Zhang Y; Chen G; Mao W; Ye Y; Kahkoska AR; Buse JB; Langer R; Gu Z Glucose-Responsive Insulin Patch for the Regulation of Blood Glucose in Mice and Minipigs. *Nat. Biomed. Eng* 2020, 4, 499–506. [PubMed: 32015407]
 - (14). Chen S; Matsumoto H; Moro-Oka Y; Tanaka M; Miyahara Y; Suganami T; Matsumoto A Microneedle-Array Patch Fabricated with Enzyme-Free Polymeric Components Capable of On-Demand Insulin Delivery. *Adv. Funct. Mater* 2018, 29, 1807369.
 - (15). Yu J; Qian C; Zhang Y; Cui Z; Zhu Y; Shen Q; Ligler FS; Buse JB; Gu Z Hypoxia and H₂O₂ Dual-Sensitive Vesicles for Enhanced Glucose-Responsive Insulin Delivery. *Nano Lett.* 2017, 17, 733–739. [PubMed: 28079384]
 - (16). Wang J; Ye Y; Yu J; Kahkoska AR; Zhang X; Wang C; Sun W; Corder RD; Chen Z; Khan SA; Buse JB; Gu Z Core-Shell Microneedle Gel for Self-Regulated Insulin Delivery. *ACS Nano* 2018, 12, 2466–2473. [PubMed: 29455516]
 - (17). Yu J; Zhang Y; Ye Y; DiSanto R; Sun W; Ranson D; Ligler FS; Buse JB; Gu Z Microneedle-Array Patches Loaded with Hypoxia-Sensitive Vesicles Provide Fast Glucose-Responsive Insulin Delivery. *Proc. Natl. Acad. Sci. U. S. A* 2015, 112, 8260–8265. [PubMed: 26100900]
 - (18). Hisamitsu I; Kataoka K; Okano T; Sakurai Y Glucose-Responsive Gel from Phenylborate Polymer and Poly(vinyl Alcohol): Prompt Response at Physiological pH through the Interaction of Borate with Amino Group in the Gel. *Pharm. Res* 1997, 14, 289–293. [PubMed: 9098868]
 - (19). Kataoka K; Miyazaki H; Bunya M; Okano T; Sakurai Y Totally Synthetic Polymer Gels Responding to External Glucose Concentration: Their Preparation and Application to On-Off Regulation of Insulin Release. *J. Am. Chem. Soc* 1998, 120, 12694–12695.
 - (20). Obaidat AA; Park K Characterization of Glucose Dependent Gel-Sol Phase Transition of the Polymeric Glucose-Concanavalin A Hydrogel System. *Pharm. Res* 1996, 13, 989–995. [PubMed: 8842034]
 - (21). Matsumoto A; Yoshida R; Kataoka K Glucose-Responsive Polymer Gel Bearing Phenylborate Derivative as a Glucose-Sensing Moiety Operating at the Physiological pH. *Biomacromolecules* 2004, 5, 1038–1045. [PubMed: 15132698]

- Author Manuscript
- Author Manuscript
- Author Manuscript
- Author Manuscript
- (22). Peppas NA; Huang Y; Torres-Lugo M; Ward JH; Zhang J Physicochemical Foundations and Structural Design of Hydrogels in Medicine and Biology. *Annu. Rev. Biomed. Eng* 2000, 2, 9–29. [PubMed: 11701505]
 - (23). Matsumoto A; Tanaka M; Matsumoto H; Ochi K; Moro-Oka Y; Kuwata H; Yamada H; Shirakawa I; Miyazawa T; Ishii H Synthetic “Smart Gel” Provides Glucose-Responsive Insulin Delivery in Diabetic Mice. *Sci. Adv* 2017, 3, No. eaaq0723.
 - (24). Podual K; Doyle FJ; Peppas NA Dynamic Behavior of Glucose Oxidase-Containing Microparticles of Poly (ethylene Glycol)-Grafted Cationic Hydrogels in An Environment of Changing pH. *Biomaterials* 2000, 21, 1439–1450. [PubMed: 10872773]
 - (25). Gu Z; Aimetti AA; Wang Q; Dang T; Zhang Y; Veiseh O; Cheng H; Langer RS; Anderson DG Injectable Nano-Network for Glucose-Mediated Insulin Delivery. *ACS Nano* 2013, 7, 4194–4201. [PubMed: 23638642]
 - (26). Dong Y; Wang W; Veiseh O; Appel EA; Xue K; Webber MJ; Tang B; Yang X; Weir GC; Langer R; Anderson DG Injectable and Glucose-Responsive Hydrogels Based on Boronic Acid-Glucose Complexation. *Langmuir* 2016, 32, 8743–8747. [PubMed: 27455412]
 - (27). Shiino D; Murata Y; Kataoka K; Koyama Y; Yokoyama M; Okano T; Sakurai Y Preparation and Characterization of A Glucose-Responsive Insulin-Releasing Polymer Device. *Biomaterials* 1994, 15, 121–128. [PubMed: 8011858]
 - (28). Luo L; Song R; Chen J; Zhou B; Mao X; Tang S Fluorophenylboronic Acid Substituted Chitosan for Insulin Loading and Release. *React. Funct. Polym* 2020, 146, 104435.
 - (29). Chang R; Li M; Ge S; Yang J; Sun Q; Xiong L Glucose-Responsive Biopolymer Nanoparticles Prepared by Co-Assembly of Concanavalin A and Amylopectin for Insulin Delivery. *Ind. Crops Prod* 2018, 112, 98–104.
 - (30). Chen W; Luo G; Vazquez-Gonzalez M; Cazelles RM; Sohn YS; Nechushtai R; Mandel Y; Willner I Glucose-Responsive Metal-Organic-Framework Nanoparticles Act as “Smart” Sense-And-Treat Carriers. *ACS Nano* 2018, 12, 7538–7545. [PubMed: 29969227]
 - (31). Fu Y; Liu W; Wang L; Zhu B; Qu M; Yang L; Sun X; Gong T; Zhang Z; Lin Q; Zhang L Erythrocyte-Membrane-Camouflaged Nanoplatform for Intravenous Glucose-Responsive Insulin Delivery. *Adv. Funct. Mater* 2018, 28, 1802250.
 - (32). Volpatti LR; Matranga MA; Cortinas AB; Delcassian D; Daniel KB; Langer R; Anderson DG Glucose-Responsive Nanoparticles for Rapid and Extended Self-Regulated Insulin Delivery. *ACS Nano* 2020, 14, 488–497. [PubMed: 31765558]
 - (33). Xiao Y; Sun H; Du J Sugar-Breathing Glycopolymersomes for Regulating Glucose Level. *J. Am. Chem. Soc* 2017, 139, 7640–7647. [PubMed: 28508651]
 - (34). Xiao Y; Hu Y; Du J Controlling Blood Sugar Levels with A Glycopolymersome. *Mater. Horiz* 2019, 6, 2047–2055.
 - (35). Zhao Y; Trewyn BG; Slowing II; Lin VS Mesoporous Silica Nanoparticle-Based Double Drug Delivery System for Glucose-Responsive Controlled Release of Insulin and Cyclic Amp. *J. Am. Chem. Soc* 2009, 131, 8398–8400. [PubMed: 19476380]
 - (36). Gu Z; Dang TT; Ma M; Tang BC; Cheng H; Jiang S; Dong Y; Zhang Y; Anderson DG Glucose-Responsive Microgels Integrated with Enzyme Nanocapsules for Closed-Loop Insulin Delivery. *ACS Nano* 2013, 7, 6758–6766. [PubMed: 23834678]
 - (37). Gordijo CR; Shuhendler AJ; Wu X Glucose-Responsive Bioinorganic Nanohybrid Membrane for Self-Regulated Insulin Release. *Adv. Funct. Mater* 2010, 20, 1404–1412.
 - (38). Duan Y; Ye F; Huang Y; Qin Y; He C; Zhao S One-Pot Synthesis of A Metal-Organic Framework-Based Drug Carrier for Intelligent Glucose-Responsive Insulin Delivery. *Chem. Commun* 2018, 54, 5377–5380.
 - (39). Kitano S; Koyama Y; Kataoka K; Okano T; Sakurai Y A Novel Drug Delivery System Utilizing A Glucose Responsive Polymer Complex between Poly (vinyl Alcohol) and Poly (N-Vinyl-2-Pyrrolidone) with a Phenylboronic Acid Moiety. *J. Controlled Release* 1992, 19, 161–170.
 - (40). Wang J; Yu J; Zhang Y; Zhang X; Kahkoska AR; Chen G; Wang Z; Sun W; Cai L; Chen Z; Qian C; Shen Q; Khademhosseini A; Buse JB; Gu Z Charge-Switchable Polymeric Complex for Glucose-Responsive Insulin Delivery in Mice and Pigs. *Sci. Adv* 2019, 5, No. eaaw4357.

- (41). Chen Z; Wang J; Sun W; Archibong E; Kahkoska AR; Zhang X; Lu Y; Ligler FS; Buse JB; Gu Z Synthetic Beta Cells for Fusion-Mediated Dynamic Insulin Secretion. *Nat. Chem. Biol* 2018, 14, 86–93. [PubMed: 29083418]
- (42). Yu J; Zhang Y; Wang J; Wen D; Kahkoska AR; Buse JB; Gu Z Glucose-Responsive Oral Insulin Delivery for Postprandial Glycemic Regulation. *Nano Res.* 2019, 12, 1539–1545.
- (43). Wang C; Ye Y; Sun W; Yu J; Wang J; Lawrence DS; Buse JB; Gu Z Red Blood Cells for Glucose-Responsive Insulin Delivery. *Adv. Mater* 2017, 29, 1606617.
- (44). Yang R; Wu M; Lin S; Nargund RP; Li X; Kelly T; Yan L; Dai G; Qian Y; Dallas-Yang Q; Fischer PA; Cui Y; Shen X; Huo P; Feng D; Erion MD; Kelley DE; Mu J A Glucose-Responsive Insulin Therapy Protects Animals against Hypoglycemia. *JCI Insight* 2018, 3, No. e97476.
- (45). Wang J; Yu J; Zhang Y; Kahkoska AR; Wang Z; Fang J; Whitelegge JP; Li S; Buse JB; Gu Z Glucose Transporter Inhibitor-Conjugated Insulin Mitigates Hypoglycemia. *Proc. Natl. Acad. Sci. U. S. A* 2019, 116, 10744–10748. [PubMed: 31097579]
- (46). Chou DH; Webber MJ; Tang B; Lin AB; Thapa LS; Deng D; Truong JV; Cortinas AB; Langer R; Anderson DG Glucose-Responsive Insulin Activity by Covalent Modification with Aliphatic Phenylboronic Acid Conjugates. *Proc. Natl. Acad. Sci. U. S. A* 2015, 112, 2401–2406. [PubMed: 25675515]
- (47). Barkai U; Weir GC; Colton CK; Ludwig B; Bornstein SR; Brendel MD; Neufeld T; Bremer C; Leon A; Evron Y; Yavriyants K; Azarov D; Zimmermann B; Maimon S; Shabtay N; Balyura M; Rozenshtein T; Vardi P; Bloch K; de Vos P; et al. Enhanced Oxygen Supply Improves Islet Viability in a New Bioartificial Pancreas. *Cell Transplant.* 2013, 22, 1463–1476. [PubMed: 23043896]
- (48). Chang R; Faleo G; Russ HA; Parent AV; Elledge SK; Bernards DA; Allen JL; Villanueva K; Hebrok M; Tang Q; Desai TA Nanoporous Immunoprotective Device for Stem-Cell-Derived Beta-Cell Replacement Therapy. *ACS Nano* 2017, 11, 7747–7757. [PubMed: 28763191]
- (49). Matsumoto A; Ishii T; Nishida J; Matsumoto H; Kataoka K; Miyahara Y A Synthetic Approach toward a Self-Regulated Insulin Delivery System. *Angew. Chem., Int. Ed* 2012, 51, 2124–2128.
- (50). Wintersteiner O; Abramson HA The Isoelectric Point of Insulin - Electrical Properties of Adsorbed and Crystalline Insulin. *J. Biol. Chem* 1933, 99, 741–753.
- (51). Insua I; Wilkinson A; Fernandez-Trillo F Polyion Complex (Pic) Particles: Preparation and Biomedical Applications. *Eur. Polym. J* 2016, 81, 198–215. [PubMed: 27524831]
- (52). Bechaouch S; Gachard I; Coutin B; Sekiguchi H Synthesis and Degradation of Nonpeptidic A-Amino Acid-Containing Polyamides. *Polym. Bull* 1997, 38, 365–370.
- (53). Quong D; Yeo JN; Neufeld RJ Stability of Chitosan and Poly-L-lysine Membranes Coating DNA-Alginate Beads When Exposed to Hydrolytic Enzymes. *J. Microencapsulation* 1999, 16, 73–82. [PubMed: 9972504]
- (54). Ren L; Liu Z; Liu Y; Dou P; Chen H Ring-Opening Polymerization with Synergistic Co-Monomers: Access to a Boronate-Functionalized Polymeric Monolith for the Specific Capture of Cis-Diol-Containing Biomolecules under Neutral Conditions. *Angew. Chem., Int. Ed* 2009, 48, 6704–6707.
- (55). Liang L; Liu Z A Self-Assembled Molecular Team of Boronic Acids at the Gold Surface for Specific Capture of Cis-Diol Biomolecules at Neutral pH. *Chem. Commun* 2011, 47, 2255–2257.

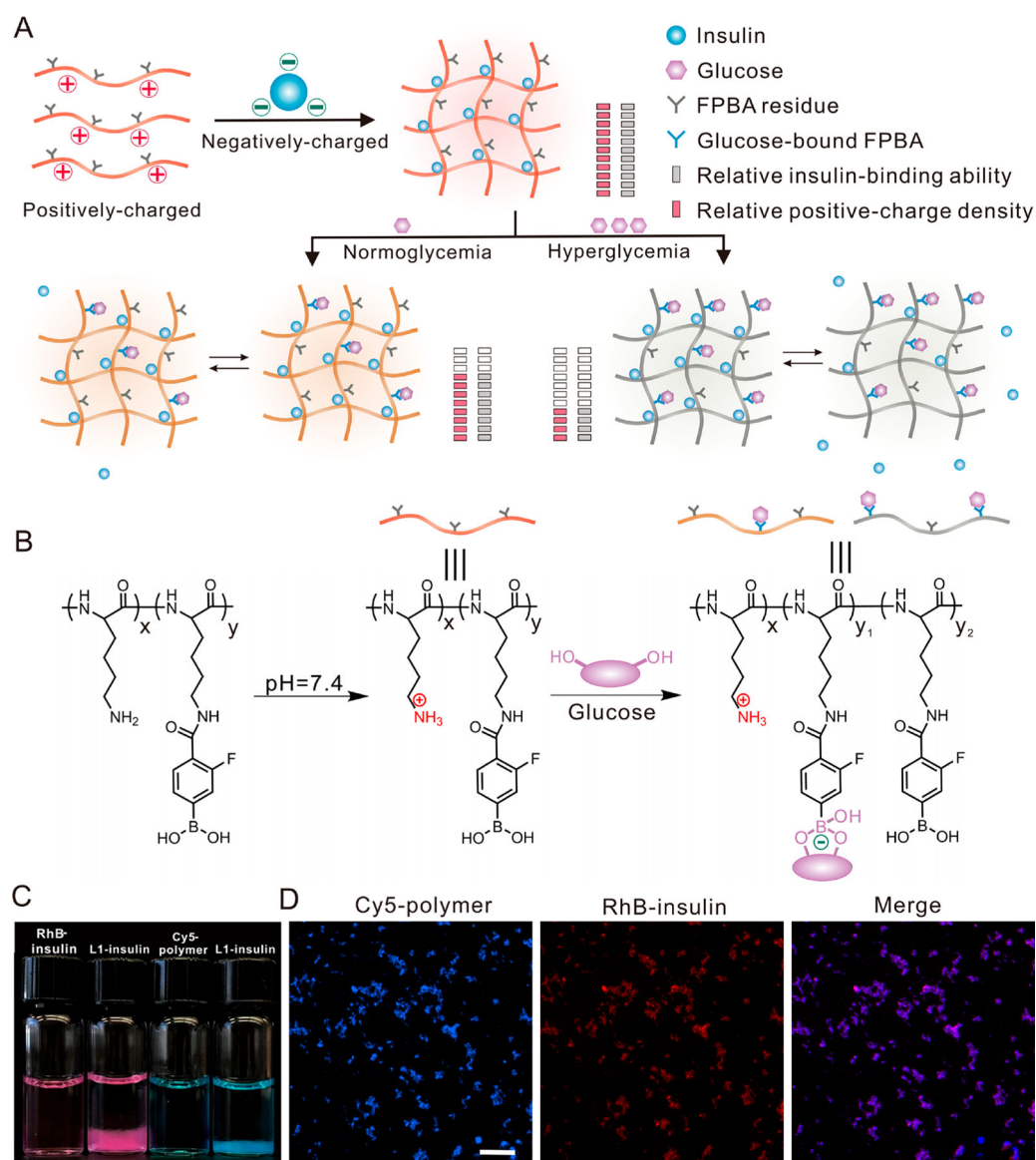
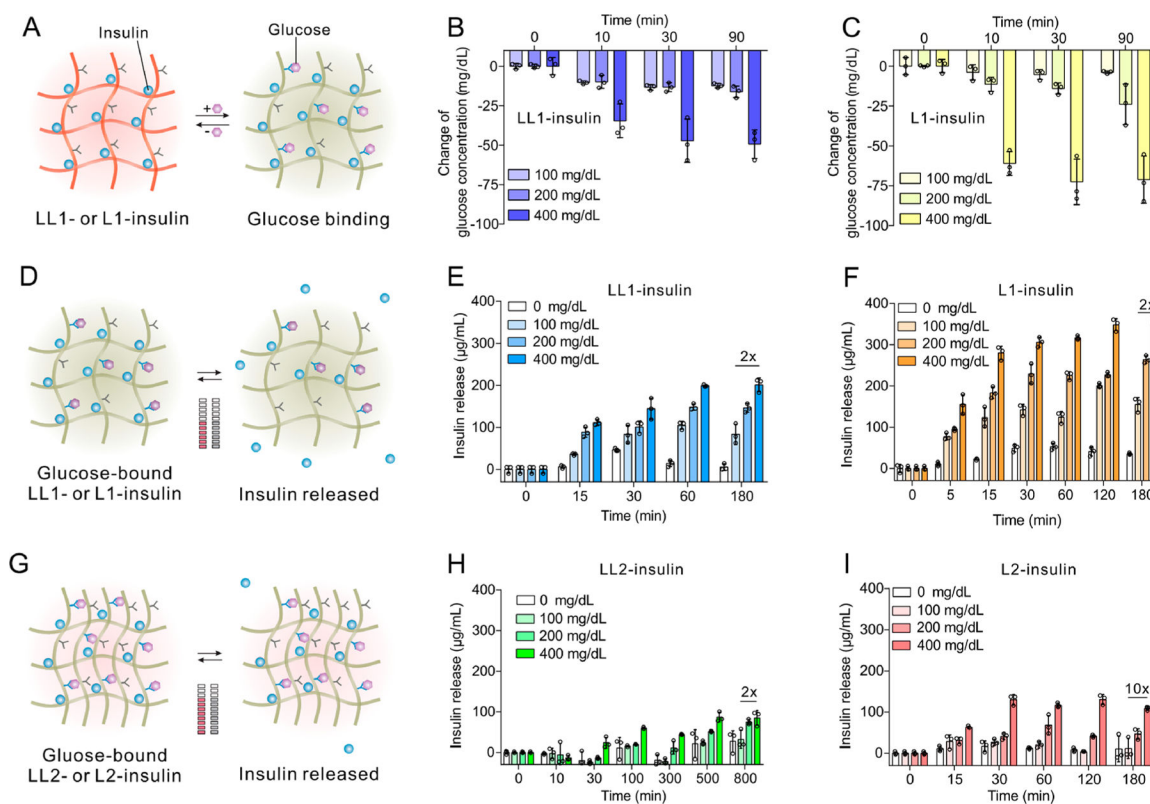
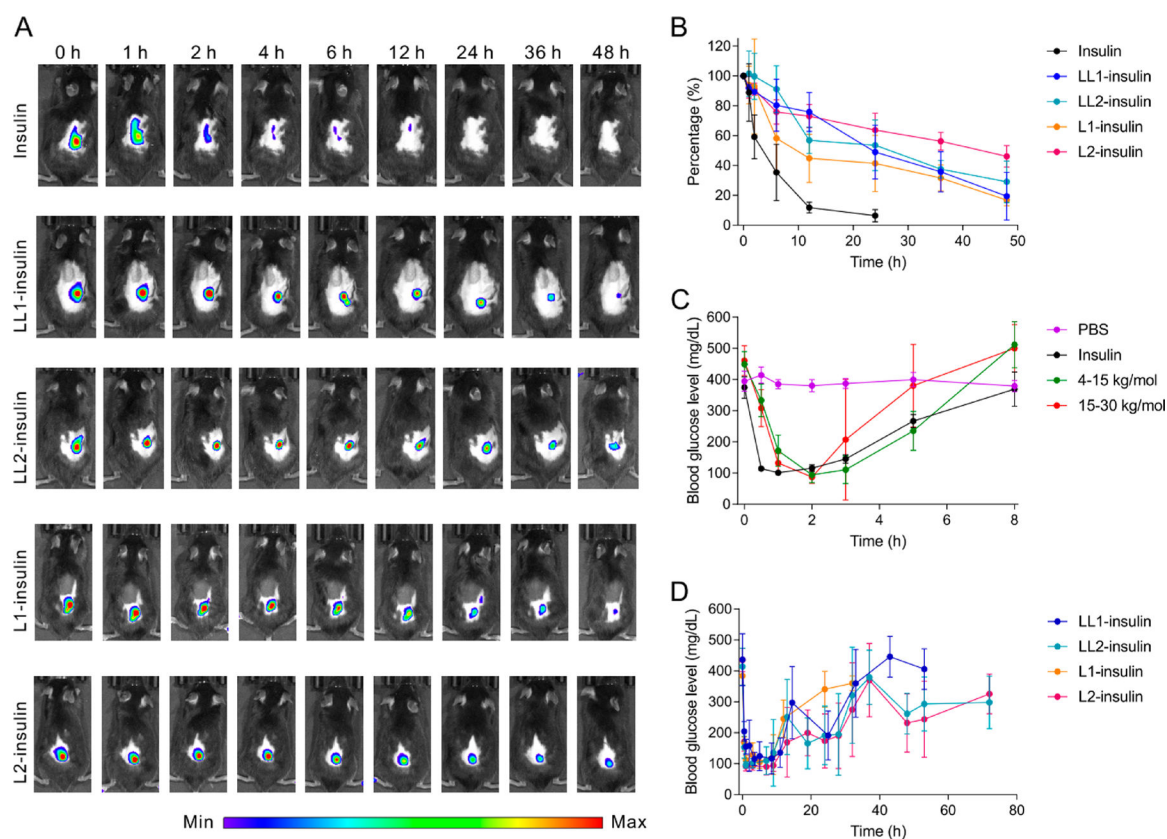


Figure 1.

Glucose-responsive complex for insulin delivery. (A,B) Schematic of the formation of the complex and mechanism of glucose-responsive insulin release. The positively charged polymer with a glucose-sensing element forms complex with the negatively charged insulin. The binding between glucose and FPBA decreases the pK_a of FPBA, introduces a negative charge, weakens the attraction between polymer and insulin, and consequently stimulates the insulin release and shifts the equilibrium to free insulin. The structure of the polymer is shown in (B). (C) Representative images of the RhB-insulin and Cy5-labeled PLL_{0.4}-FPBA_{0.6} before and after forming complexes. The complex was prepared from either Rhodamine B-labeled insulin (red) and unlabeled polymer or cyanine 5 (Cy5)-labeled PLL_{0.4}-FPBA_{0.6} (blue) and unlabeled insulin. Insulin and polymer were used in equal weight. (D) Representative fluorescence images of the complex. Cy5-labeled PLL_{0.4}-FPBA_{0.6} and RhB-insulin are shown in blue and red, respectively. Scale bar, 100 μm .

**Figure 2.**

In vitro glucose-responsive insulin release. (A–C) Schematic and glucose binding of insulin complexes. The glucose binds to the FPBA residues in polymers and leads to decreased glucose concentration in solution. The complexes were prepared from an equal weight of insulin and PLL_{0.65}-FPBA_{0.35} (LL1-insulin, B) and PLL_{0.4}-FPBA_{0.6} (L1-insulin, C), respectively. PLL used here had a MW of 30–70 kg/mol. The glucose concentration was measured using a glucose meter (Clarity). (D–F) Schematic and the glucose-responsive insulin release from complexes. The complex was prepared from an equal weight of insulin and either PLL_{0.65}-FPBA_{0.35} (LL1-insulin, E) or PLL_{0.4}-FPBA_{0.6} (L1-insulin, F). LL1 and L1 had N/C ratios of 3.5 and 2.1, respectively (see Supporting Information, Table S1). The glucose binding to FPBA weakened the attraction and liberated insulin from the complex into the solution. (G–I) Schematic and glucose-responsive insulin release from complexes. The complexes were prepared from insulin and either PLL_{0.65}-FPBA_{0.35} (LL2-insulin, H) or PLL_{0.4}-FPBA_{0.6} (L2-insulin, I) of double weight. LL2 and L2 had N/C ratios of 6.3 and 3.6, respectively (see Supporting Information, Table S1). Data are mean ± SD ($n = 3$). SD, standard deviation.

**Figure 3.**

In vivo studies in type 1 diabetic mice. (A) Representative IVIS images of mice after treated with insulin and various insulin complexes. Insulin was labeled with Cy5. (B) Quantification of fluorescence intensity in (A). Data are mean \pm SD ($n = 3$). (C) Blood glucose levels of diabetic mice treated with PBS, native insulin, and insulin complexes that were prepared from an equal weight of native insulin and PLL_{0.57}-FPBA_{0.43} with the original PLL MW of 4–15 kg/mol or PLL_{0.6}-FPBA_{0.4} with original PLL MW of 15–30 kg/mol. Data are mean \pm SD ($n = 5$ to 10). (D) Blood glucose levels of diabetic mice treated with LL1-insulin, LL2-insulin, L1-insulin, and L2-insulin, with PLL having an original MW of 30–70 kg/mol. The insulin-equivalent dose was set to 1.5 mg/kg. Data are mean \pm SD ($n = 5$ to 10).

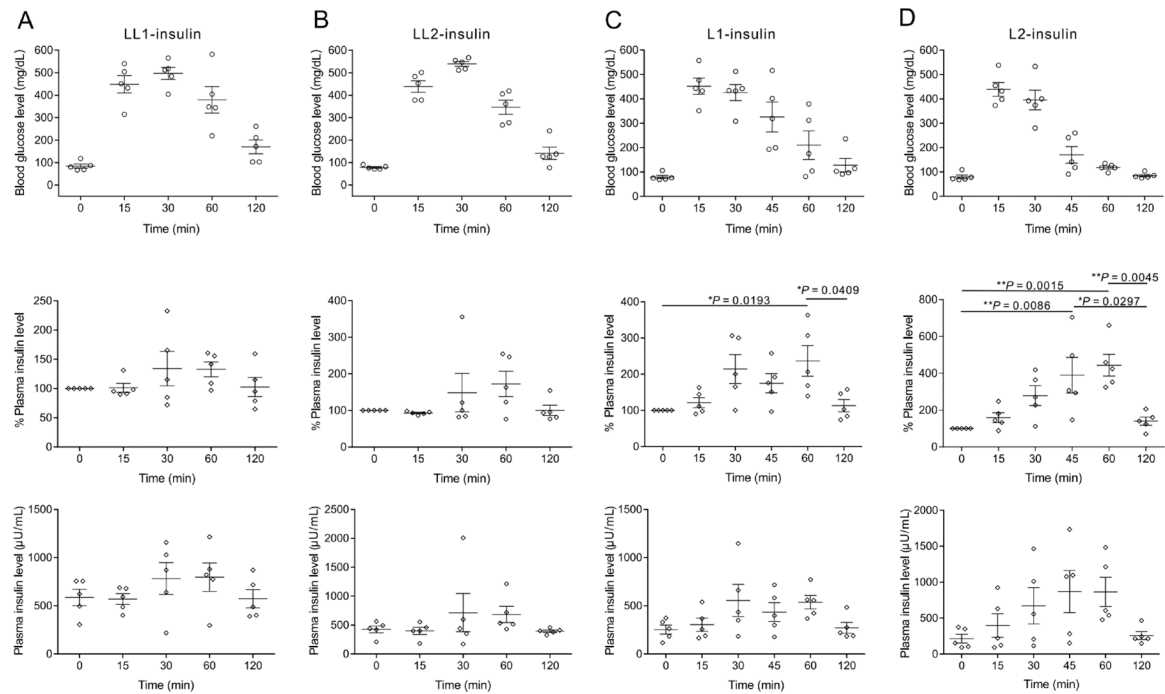


Figure 4.

Plasma insulin level change associated with intraperitoneal glucose tolerance test in diabetic mice. The diabetic mice were treated with LL1-insulin (A), LL2-insulin (B), L1-insulin (C), and L2-insulin (D), respectively. The insulin-equivalent dose was set to 1.5 mg/kg. The glucose (3 g/kg) was given at 8 h post-treatment with complexes. The plasma insulin level of each mouse just before treatment was set as 100%. The 0 min time point was set at the time of glucose injection. Data are mean \pm SEM ($n = 5$). One-way ANOVA with Tukey post-hoc tests were used to carry out multiple comparisons. * $P < 0.05$; ** $P < 0.01$.

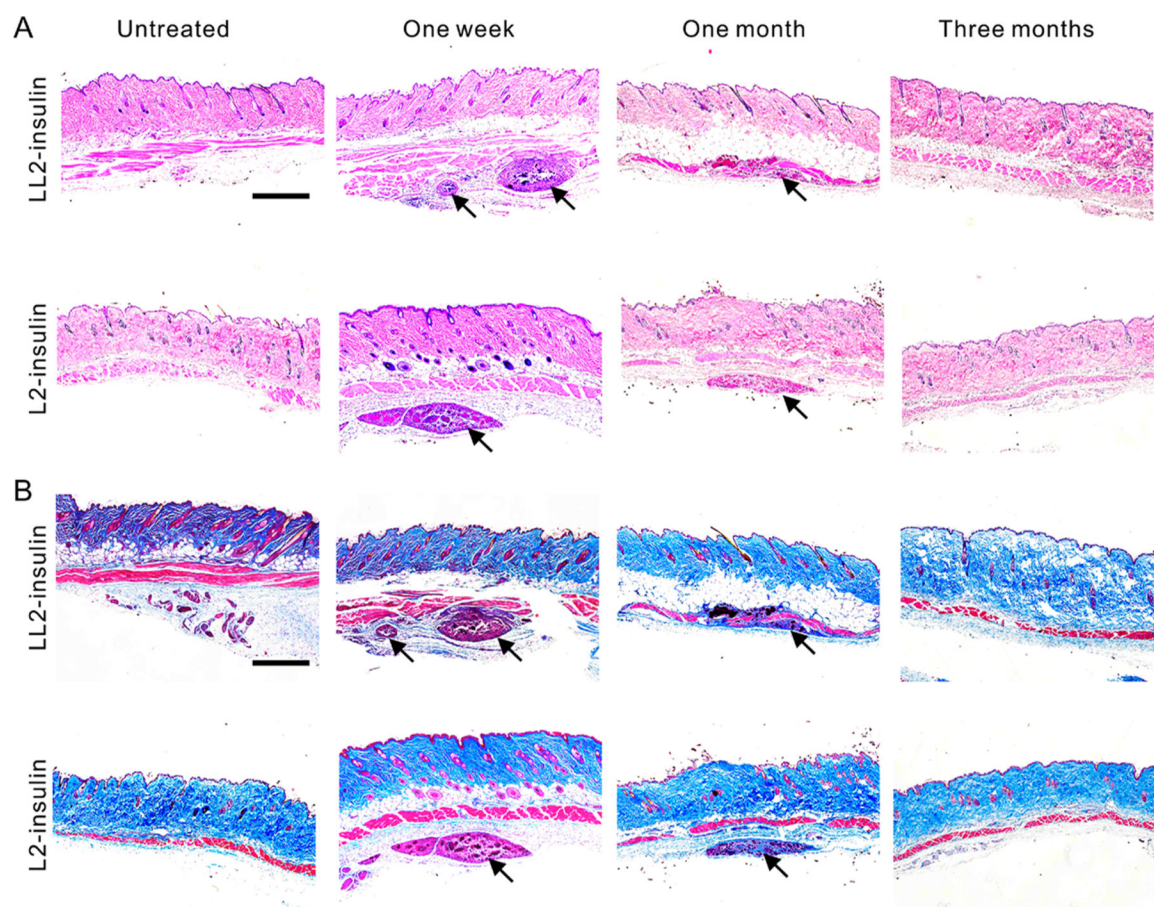


Figure 5. Representative images of H&E or Masson's trichrome staining sections. Diabetic mice were injected with various complexes and the skins at the treatment sites were obtained between time intervals. H&E staining (A) and Masson's trichrome staining (B) were performed. The images were taken on a microscope (Nikon, Ti-U). The skins without treatment were used as control samples. Black arrows indicate the injected complexes. Scale bars, 250 μm .